DOI 10.2478/ama-2024-0064 acta mechanica et automatica, vol.18 no.4 (2024)

THE CONSTRUCTION OF ANALYTICAL EXACT SOLITON WAVES OF KURALAY EQUATION

Waqas Ali FARIDI*, Muhammad ABU BAKAR*, Zhaidary MYRZAKULOVA, Ratbay MYRZAKULOV**, Mawahib ELAMIN***, Lakhdar RAGOUB****, Lanre AKINYEMI*****

*Department of Mathematics, University of Management and Technology, Lahore, Pakistan
**Ratbay Myrzakulov Eurasian International Centre for Theoretical Physics, Astana, Kazakhstan
***Department of Mathematics, College of Science, Qassim University, Buraydah, 51452, Saudi Arabia
****Mathematics Department, University of Prince Mugrin, P.O. Box 41040, Al Madinah 42241, Saudi Arabia
*****Department of Mathematics, Hampton University, Hampton, Virginia, USA

Wa966142@gmail.com, m.abubakar055@gmail.com, zrmyrzakulova@gmail.com, myrzakuloy.r@enu.kz, ma.elhag@qu.edu.sa, l.ragoub@upm.edu.sa, lanre.akinyemi@hamptonu.edu

received 30 August 2023, revised 12 October 2023, accepted 18 October 2023

Abstract: The primary objective of this work is to examine the Kuralay equation, which is a complex integrable coupled system, in order to investigate the integrable motion of induced curves. The soliton solutions derived from the Kuralay equation are thought to be the supremacy study of numerous significant phenomena and extensive applications across a wide range of domains, including optical fibres, nonlinear optics and ferromagnetic materials. The inverse scattering transform is unable to resolve the Cauchy problem for this equation, so the analytical method is used to produce exact travelling wave solutions. The modified auxiliary equation and Sardar sub-equation approaches are used to find solitary wave solutions. As a result, singular, mixed singular, periodic, mixed trigonometric, complex combo, trigonometric, mixed hyperbolic, plane and combined bright–dark soliton solution can be obtained. The derived solutions are graphically displayed in 2-D and 3-D glances to demonstrate how the fitting values of the system parameters can be used to predict the behavioural responses to pulse propagation. This study also provides a rich platform for further investigation.

Key words: The Kuralay equation; modified auxiliary equation method; analytical solitary wave solutions

1. INTRODUCTION

As technology advances, partial differential equations (PDEs) have proven to be an essential tool for scientists and researchers for understanding physical phenomena. By employing various methodologies and technologies, they have achieved a higher level of precision in examining the structures of various physical phenomena. The use of nonlinear partial differential equations (NLPDEs) is particularly valuable in modelling nonlinear phenomena in various applied as well as in natural sciences, such as acoustics physics, plasma and solid-state physics. These equations provide an in-depth and clear understanding of the observed physical phenomena, allowing for precise predictions of their future propagation. Furthermore, use of NLPDEs in travelling wave profile's analysis has an impact as an invaluable tool in a variety of fields, ranging from quantum mechanics and fluid mechanics to different fields in engineering. Consequently, a multitude of researchers have delved into diverse nonlinear partial differential models, aiming to attain a more profound understanding of the dynamics exhibited by the examined physical phenomena. Recent examinations have encompassed investigations of Date–Jimbo–Kashiwara–Miwa equation [1–3], Riemann wave equation [4,5], Schrödinger equation [6–11], Navier–Stokes equations [12–15], Lakshmanan–Porsezian–Daniel equation [16,17], Chen–Lee–Liu dynamical equation [18–21] and many others [22–30].

Many researchers have paid attention to the field of analytical solutions. Kumar and Niwas have discussed the dynamical aspects and constructed the soliton solutions of the distinct governing models [31–33]. El-Ganaini et al. [34] utilised the Lie symmetry approach and analytical method to develop the invariant solutions. Kumar et al. [35] investigated the Kudryashov–Sinelshchikov equation by using the generalised exponential rational function (GERF) method. Abdou et al. [36] applied the he generalised Kudryashov (GK) approach and the sine–Gordon expansion approach to the deoxyribonucleic acid model for constructing new specific analytical solutions. Kumar and Kumar [37] executed the GERF method to construct numerous and large numbers of exact analytical solitary wave solutions of the nonlinear extended Zakharov–Kuznetsov equation. Mathanaranjan [38,39] has developed the soliton solutions by using analytical techniques. Zhao et al. [40] applied a new GERF method on the nonlinear wave model and constructed the analytical solutions. Mathanaranjan et al. [41] utilised the extended sine–Gordon equation expansion method and developed the soliton solutions. Mathanaranjan and Vijayakumar [42] discussed the fractional soliton solutions by executing the analytical solutions. Mathanaranjan et al. [43] generated the chirped optical solitons and examined the stability analysis of the nonlinear Schrödinger equation.

Furthermore, an area witnessing a notable surge in the application of NLPDEs is the exploration of soliton waves (distinct wave formations that uphold their form and speed throughout propagation). Diverse nonlinear physical models are being employed by researchers on solitons waves to comprehend and prognosticate their propagation. Consequently, these waves have gained escalating significance across various domains like optical fibres, nonlinear optics and ferromagnetic materials. Recent accomplishments in the exploration of soliton waves are documented in Refs [44–49]. By cultivating a deeper comprehension of soliton waves, scholars can propel advancements in these realms and uncover novel applications.

The integrable complex coupled Kuralay governing system (K-IIE) as referenced in [50] is as follows:

$$\iota\mathbb{K}_t - \mathbb{K}_{xt} - \mathbb{V}\mathbb{K} = 0$$
$$\iota\mathbb{R}_t + \mathbb{R}_{xt} + \mathbb{V}\mathbb{K} = 0,$$
$$\mathbb{V}_x + 2d^2(\mathbb{R}\mathbb{K})_t = 0. \tag{1}$$

In this context, *K (x, t)* signifies a complex function, accompanied by its corresponding complex conjugate denoted as *K (x, t).* In contrast, V stands for a real potential function conditional upon the autonomous spatial 'x' and temporal variables 't'. Furthermore, the (K-IIE) equation incorporates two supplementary variations, specifically (K-IIAE) and (K-IIBE) [51–53].

Assuming d = 1 and R = $\epsilon\overline{K}$, where ϵ = ±1, the aforementioned equation system transforms into:

$$\iota\mathbb{K}_t - \mathbb{K}_{xt} - \mathbb{V}\mathbb{K} = 0,$$
$$\mathbb{V}_x - 2\epsilon(|\mathbb{K}|^2)_t = 0. \tag{2}$$

Recently (2023), Mathanaranjan [54] applied F-expansion and new extended auxiliary equation methods and constructed the solitary waves and elliptic function solutions of Kuralay equation. Many novel solutions have been generated, other dynamical aspects analysed and the conserved quantities of the Kuralay equation developed. However, many solutions and families were missing such as periodic patterns featuring elevated crests and troughs, as well as anti-peaked crests and troughs, periodic kinks, anti-kinks and compactons in both bright and dark forms. Thus, in order to fill this gap, this study is carried out utilising the modified auxiliary equation and Sardar sub-equation method.

Apart from the benefits associated with employing NLPDEs, the quest for precise analytical solutions to these equations presents challenges. To tackle this, a variety of techniques have been formulated. These approaches encompass the inverse scattering method [55], variational iteration method [56,57], integral scheme [58], soliton perturbation theory [59], positive quadratic function method [60], (G'/G2)-expansion method [61] and Lie symmetry approach [62], among others. This article investigates soliton solutions for the (K-IIE) equation by employing two distinctive methodologies: the modified auxiliary equation method [63] and the Sardar sub-equation approach [64]. Employing these methodologies results in a broad spectrum of solutions, spanning rational, trigonometric and hyperbolic manifestations.

The techniques described in Section (2) are explained in this article. The solutions derived from the model are then examined in Section (3), where various parameter values acquired using the used approaches are used. The presentation of graphical representations is also included in this section. Section (4) involves a visual evaluation of the solutions and the article concludes in Section (5), with a summary of the results.

2. DESCRIPTION OF ANALYTICAL METHODS

Consider an NLPDE of the following form:

$$Y(\mathbb{U}, \mathbb{U}_t, \mathbb{U}_x, \mathbb{U}_{tt}, \mathbb{U}_{xx}, \cdots) = 0. \tag{3}$$

Its NODE will be:

$$\mathbb{Q}(\mathbb{R}, \mathbb{R}', \mathbb{R}'', \cdots) = 0. \tag{4}$$

Consider:

$$\mathbb{U}(x,t) = \mathbb{U}(\Omega) \tag{5}$$

where Ω = *mx* + *ct*. The prime notations within Eq. (4) signify the differentiation order concerning distinct variables within the equation.

2.1. Modified auxiliary equation method

Utilising the MAE approach [63], we can regard the subsequent equation as the general solution for Eq. (4):

$$\mathbb{U}(\Omega) = \alpha_0 + \sum_{i=1}^{N} [\alpha_i(z^{h(\Omega)} + \beta_i z^{-h(\Omega)}] \tag{6}$$

$\alpha_i s$, $\beta_i s$ are constants of the equation and Ω = *k1(x + y) +* $k_2 t$. The function *h(Ω)* can be described by the auxiliary equation that follows:

$$h'(\Omega) = \frac{\beta + \alpha z^{-h(\Omega)} + \gamma z^{h(\Omega)}}{\ln(z)} \quad . \tag{7}$$

Here, *γ, z, α* and *β* are real arbitrary constants, where *z>0* and *z≠1*. Furthermore, $\alpha_i s$ and *βis* cannot be zero at the same time.

Eq. (7) has the following solutions:

If γ ≠ 0 and Ξ < 0,

$$z^{h(\Omega)} = -\left[\frac{\beta + \sqrt{-\Xi}tan\left(\frac{\sqrt{-\Xi}\Omega}{2}\right)}{2\gamma}\right] \; or \; z^{h(\Omega)} = -\left[\frac{\beta + \sqrt{-\Xi}cot\left(\frac{\sqrt{-\Xi}\Omega}{2}\right)}{2\gamma}\right]. \tag{8}$$

If γ ≠ 0 and Ξ > 0,

$$z^{h(\Omega)} = -\left[\frac{\beta + \sqrt{\Xi}tanh\left(\frac{\sqrt{\Xi}\Omega}{2}\right)}{2\gamma}\right] \; r \; z^{h(\Omega)} = -\left[\frac{\beta + \sqrt{\Xi}coth\left(\frac{\sqrt{\Xi}\Omega}{2}\right)}{2\gamma}\right]. \tag{9}$$

If γ ≠ 0 and Ξ = 0,

$$z^{h(\Omega)} = -\left[\frac{2 + \beta\Omega}{2\gamma\Omega}\right] , \tag{10}$$

where Ξ = $\beta^2 - 4\alpha\gamma$.

2.2. Sardar sub-equation method

By employing the Sardar sub-equation approach [64], we can view the ensuing equation as the general solution for Eq. (4):

$$U(\Omega) = \sum_{i=0}^{N}\left(a_i M^i(\Omega)\right), \; 0 \le i \le N, \tag{11}$$

where a_i in Eq. (11) are real constants and M(Ω) satisfy the

$$M'(\Omega) = \sqrt{\zeta + \upsilon M(\Omega)^2 + M(\Omega)^4}, \tag{12}$$

with real constants ζ and *υ*.

Eq. (12) has the following solutions:
Case 1: if $\upsilon > 0$ and $\zeta = 0$;
ODE of the following form:

$$M_1^{\pm}(\Omega) = \pm\sqrt{-\mathrm{pq}\upsilon}\,\mathrm{sech_{pq}}\left(\sqrt{\upsilon}\Omega\right) \tag{13}$$

$$M_2^{\pm}(\Omega) = \pm\sqrt{\mathrm{pq}\upsilon}\,\mathrm{csch_{pq}}\left(\sqrt{\upsilon}\Omega\right) \tag{14}$$

where

$$sech_{pq}(\Omega) = \frac{2}{pe^{\Omega}+qe^{-\Omega}}, \quad csch_{pq}(\Omega) = \frac{2}{pe^{\Omega}-qe^{-\Omega}}.$$

Case 2: if $\upsilon < 0$ and $\zeta = 0$:

$$M_3^{\pm}(\Omega) = \pm\sqrt{-\mathrm{pq}\upsilon}\,\mathrm{sec_{pq}}\left(\sqrt{-\upsilon}\Omega\right), \tag{15}$$

$$M_4^{\pm}(\Omega) = \pm\sqrt{-\mathrm{pq}\upsilon}\,\mathrm{csc_{pq}}\left(\sqrt{-\upsilon}\Omega\right) \tag{16}$$

where

$$\mathrm{sec_{pq}}(\Omega) = \frac{2}{\mathrm{pe^{\iota\Omega}+qe^{-\iota\Omega}}}, \quad \mathrm{csc_{pq}}(\Omega) = \frac{2\iota}{\mathrm{pe^{\iota\Omega}-qe^{-\iota\Omega}}}.$$

Case 3: if $\upsilon < 0$ and $\zeta = \frac{\upsilon^2}{4}$:

$$M_5^{\pm}(\Omega) = \pm\sqrt{-\frac{\upsilon}{2}}\,\mathrm{tanh_{pq}}\left(\sqrt{-\frac{\upsilon}{2}}\Omega\right), \tag{17}$$

$$M_6^{\pm}(\Omega) = \pm\sqrt{-\frac{\upsilon}{2}}\,\mathrm{coth_{pq}}\left(\sqrt{-\frac{\upsilon}{2}}\Omega\right), \tag{18}$$

$$M_7^{\pm}(\Omega) = \pm\sqrt{-\frac{\upsilon}{2}}\left(\mathrm{tanh_{pq}}\left(\sqrt{-2\upsilon}\Omega\right) \pm \iota\sqrt{\mathrm{pq}}\,\mathrm{sech_{pq}}\left(\sqrt{-2\upsilon}\Omega\right)\right), \tag{19}$$

$$M_8^{\pm}(\Omega) = \pm\sqrt{-\frac{\upsilon}{2}}\left(\mathrm{coth_{pq}}\left(\sqrt{-2\upsilon}\Omega\right) \pm \sqrt{\mathrm{pq}}\,\mathrm{csch_{pq}}\left(\sqrt{-2\upsilon}\Omega\right)\right), \tag{20}$$

$$M_9^{\pm}(\Omega) = \pm\sqrt{-\frac{\upsilon}{8}}\left(\mathrm{tanh_{pq}}\left(\sqrt{-\frac{\upsilon}{8}}\Omega\right) + \mathrm{coth_{pq}}\left(\sqrt{-\frac{\upsilon}{8}}\Omega\right)\right), \tag{21}$$

where

$$\tanh_{pq}(\Omega) = \frac{pe^{\Omega} - qe^{-\iota\Omega}}{pe^{\iota\Omega} + qe^{-\iota\Omega}},$$

$$\coth_{pq}(\Omega) = \frac{pe^{\iota\Omega}+qe^{-\iota\Omega}}{pe^{\iota\Omega}-qe^{-\iota\Omega}}.$$

Case 4: if $\upsilon > 0$ and $\zeta = \frac{\upsilon^2}{4}$:;

$$M_{10}^{\pm}(\Omega) = \pm\sqrt{\frac{\upsilon}{2}}\,\mathrm{tan_{pq}}\left(\sqrt{\frac{\upsilon}{2}}\Omega\right), \tag{22}$$

$$M_{11}^{\pm}\Omega = \pm\sqrt{\frac{\upsilon}{2}}\,\mathrm{cot_{pq}}\left(\sqrt{\frac{\upsilon}{2}}\Omega\right), \tag{23}$$

$$M_{12}^{\pm}(\Omega) = \pm\sqrt{\frac{\upsilon}{2}}\left(\mathrm{tan_{pq}}\left(\sqrt{2\upsilon}\Omega\right) \pm \sqrt{\mathrm{pq}}\,\mathrm{sec_{pq}}\left(\sqrt{2\upsilon}\Omega\right)\right), \tag{24}$$

$$M_{13}^{\pm}(\Omega) = \pm\sqrt{\frac{\upsilon}{2}}\left(\mathrm{cot_{pq}}\left(\sqrt{2\upsilon}\Omega\right) \pm \sqrt{\mathrm{pq}}\,\mathrm{csch_{pq}}\left(\sqrt{2\upsilon}\Omega\right)\right), \tag{25}$$

$$M_{14}^{\pm}(\Omega) = \pm\sqrt{\frac{\upsilon}{8}}\left(\mathrm{tan_{pq}}\left(\sqrt{\frac{\upsilon}{8}}\Omega\right) + \mathrm{cot_{pq}}\left(\sqrt{\frac{\upsilon}{8}}\Omega\right)\right), \tag{26}$$

where

$$\tanh_{pq}(\Omega) = -\iota\frac{pe^{\Omega} - qe^{-\iota\Omega}}{pe^{\iota\Omega} + qe^{-\iota\Omega}},$$

$$\coth_{pq}(\Omega) = \iota\frac{pe^{\iota\Omega}+qe^{-\iota\Omega}}{pe^{\iota\Omega}-qe^{-\iota\Omega}}.$$

The functions mentioned are trigonometric and hyperbolic functions that have parameters represented by p and q. When p and q are both equal to 1, these functions become the known trigonometric and hyperbolic functions.

3. THE FORMULATION OF SOLITON SOLUTION OF KURALAY EQUATION

This section includes the presentation of the soliton solution, along with graphical representations that illustrate these solutions for the model being studied.

Now, in order to find the soliton solutions, the travelling wave transformation will be used, which is given as follows:

$$\mathbb{K}(x,t) = \mathbb{U}(\Omega)e^{\iota(kx+wt+\eta)},$$
$$\mathbb{V}(x,t) = \mathbb{V}(\Omega)e^{\iota(kx+wt+\eta)},$$
$$\Omega = mx + ct. \tag{27}$$

Thus,

$$\mathbb{K}_t = (c\mathbb{U}' + \iota w\mathbb{U})e^{\iota(kx+wt+\eta)},$$
$$\mathbb{K}_x = (m\mathbb{U}' + \iota k\mathbb{U})e^{\iota(kx+wt+\eta)}, \tag{28}$$
$$\mathbb{K}_{xt} = (cm\mathbb{U}'' + \iota wm\mathbb{U}' + \iota ck\mathbb{U}' + \iota kw\mathbb{U})e^{\iota(kx+wt+\eta)}.$$

Eqs (27) and (28) are substituted into Eq. (2) and the following is obtained:

$$\iota(c\mathbb{U}' + \iota w\mathbb{U}) - (cm\mathbb{U}'' + \iota wm\mathbb{U}' + iotack\mathbb{U}' - kw\mathbb{U}) - \mathbb{V}\mathbb{U} = 0,$$
$$m\mathbb{V}' - 4\upsilon c\mathbb{U}\mathbb{U}' = 0. \tag{29}$$

On integrating the second part of Eq. (29)

$$V = \frac{2\upsilon cU^{\mathbb{2}}}{m} - \frac{c_1}{m}.. \tag{30}$$

Eq. (30) is plugged into Eq. (29) and we obtain as follows:

$$\iota(cU' + \iota wU) - (cmU'' + \iota wmU' + \iota ckU' - wU) - \left(\frac{2\upsilon cU^{\mathbb{2}}}{m} - \right)U = 0, \tag{31}$$

where $\mathrm{n} = \frac{\mathrm{c}}{\mathrm{m}}$. The real and imaginary parts of Eq. (31) are given, respectively, as

$$U'' + \frac{(w(1-k)-n)}{cm}U + \frac{2\upsilon U^{\mathbb{3}}}{m^2} = 0, \tag{32}$$

$$(c - wm - ck)\mathbb{U}' = 0. \tag{33}$$

From the imaginary part (Eq. (33)) is implied the following value of m:

$$m = \frac{c(k-1)}{w}. \tag{34}$$

By plugging Eq. (34) into Eq. (32), we obtain as follows:

$$U'' + \frac{w(w(1-k)-n)}{c^2(k-1)}U + \frac{2w^2\upsilon U^{\mathbb{3}}}{c^2(k-1)^2} = 0. \tag{35}$$

DOI 10.2478/ama-2024-0064

3.1. Solution by applying MAE method

The solution using the MAE method for Eq. (35) can be expressed as follows, after determining the homogeneous balancing constant N = 1:

$$\mathbb{U}(\Omega)=\alpha_0+\alpha_1 z^{h(\Omega)}+\beta_1 z^{-h(\Omega)}. \quad (36)$$

To obtain the system of equations, the solution from Eq. (36) was substituted into Eq. (35), and the varying power coefficients of zh(Ω) were calculated. The algebraic equation system that was obtained was then solved using the Mathematica software, which resulted in four distinct families of values for α0, α1 and β1. By using each family of values separately, the following solutions are obtained:

3.1.1. Family 1

$$\alpha_0=\pm\frac{\beta\sqrt{(k-1)(kw+n-w)}}{\sqrt{2w\epsilon\Xi}},\ \alpha_1=\pm\frac{2\gamma\sqrt{(k-1)(kw+n-w)}}{\sqrt{2w\epsilon\Xi}},\beta_1=0,\ c=\pm\frac{\sqrt{2}\sqrt{w((k-1)w+n)}}{\sqrt{((1-k)\Xi)}}, \quad (37)$$

General solution for family 1,

$$U(\Omega)=\pm\frac{\sqrt{(k-1)(kw+n-w)}}{\sqrt{2w\epsilon\Xi}}\left(\beta\pm 2\gamma z^{h(\Omega)}\right). \quad (38)$$

Observing that numerous solutions can be obtained by substituting Eqs (8)–(10) into Eq. (38), the resulting solutions are as follows:

Case1: If Ξ < 0, γ ≠ 0;

$$\mathbb{K}_{1,1}(x,t)=\pm\left(\frac{\sqrt{((n+(k-1)w)(1-k)}tan\left(\frac{1}{2}\Omega\sqrt{-\Xi}\right)}{\sqrt{2w\epsilon}}\right)e^{\iota(kx+et+\eta)} \quad (39)$$

$$\mathbb{V}_{1,1}(x,t)=\frac{2cv}{m}\left(\frac{\sqrt{((n+(k-1)w)(1-k)}tan\left(\frac{1}{2}\Omega\sqrt{-\Xi}\right)}{\sqrt{2w\epsilon}}\right)-\frac{c_1}{m}, \quad (40)$$

or

$$\mathbb{K}_{1,2}(x,t)=\pm\left(\frac{\sqrt{-((n+(k-1)w)(1-k)}\cot\left(\frac{1}{2}\Omega\sqrt{-\Xi}\right)}{\sqrt{2w\epsilon}}\right)e^{\iota(kx+wt+\eta)}, \quad (41)$$

$$\mathbb{V}_{1,2}(x,t)=\frac{2cv}{m}\left(\frac{\sqrt{-((n+(k-1)w)(1-k)}\cot\left(\frac{1}{2}\Omega\sqrt{-\Xi}\right)}{\sqrt{2w\epsilon}}\right)^2e^{\iota(kx+wt+\eta)}-\frac{c_1}{m}. \quad (42)$$

Case2: If Ξ > 0, γ ≠ 0;

$$\mathbb{K}_{1,3}(x,t)=\pm\left(\frac{\sqrt{((n+(k-1)w)(1-k)}tanh\left(\frac{1}{2}\Omega\sqrt{\Xi}\right)}{\sqrt{2w\epsilon}}\right)e^{\iota(kx+et+\eta)}, \quad (43)$$

$$\mathbb{V}_{1,3}(x,t)=\frac{2cv}{m}\left(\frac{\sqrt{((n+(k-1)w)(1-k)}tanh\left(\frac{1}{2}\Omega\sqrt{\Xi}\right)}{\sqrt{2w\epsilon}}\right)-\frac{c_1}{m}, \quad (44)$$

or

$$\mathbb{K}_{1,4}(x,t)=\pm\left(\frac{\sqrt{((n+(k-1)w)(1-k)}\coth\left(\frac{1}{2}\Omega\sqrt{\Xi}\right)}{\sqrt{2w\epsilon}}\right)e^{\iota(kx+wt+\eta)}, \quad (45)$$

$$\mathbb{V}_{1,4}(x,t)=\frac{2cv}{m}\left(\frac{\sqrt{((n+(k-1)w)(1-k)}\coth\left(\frac{1}{2}\Omega\sqrt{\Xi}\right)}{\sqrt{2w\epsilon}}\right)^2e^{\iota(kx+wt+\eta)}-\frac{c_1}{m}. \quad (46)$$

3.1.2. Family 2

$$\alpha_0=\pm\frac{\beta\sqrt{((n+(k-1)w)(1-k)}}{\sqrt{2w\epsilon\Xi}},\alpha_1=0,\beta_1=\pm\frac{2\alpha\sqrt{((n+(k-1)w)(1-k)}}{\sqrt{2w\epsilon\Xi}},\ c=\pm\frac{\sqrt{2}\sqrt{w((k-1)w+n)}}{\sqrt{((1-k)(\Xi))}}. \quad (47)$$

General solution for family 2,

$$U(\Omega)=\frac{\beta\sqrt{((n+(k-1)w)(1-k)\}}}{\sqrt{2w\epsilon\Xi}}\pm\frac{2\alpha z^{-h(\Omega)}\sqrt{(k-1)(kw+n-w)}}{\sqrt{2w\epsilon\Xi}} \quad (48)$$

It is observed that numerous solutions can be obtained by substituting equations Eq. (8)–(10) into Eq. (48). The resulting solutions are as follows:

Case1 : If γ≠0, Ξ < 0;

$$\mathbb{K}_{2,1}(x,t)=\pm\left(\frac{\sqrt{((n+(k-1)w)(1-k)}(\beta(\sqrt{-\Xi}\tan(\frac{1}{2}\Omega\sqrt{-\Xi})+\beta)-4\alpha\gamma)}{(\sqrt{-\Xi}\tan(\frac{1}{2}\Omega\sqrt{-\Xi})+\beta)\sqrt{2w\epsilon(\Xi)}}\right)e^{\iota(kx+et+\eta)}, \quad (49)$$

$$\mathbb{V}_{2,1}(x,t)=\frac{2cv}{m}\left(\frac{\sqrt{((n+(k-1)w)(1-k)}(\beta(\sqrt{-\Xi}\tan(\frac{1}{2}\Omega\sqrt{-\Xi})+\beta)-4\alpha\gamma)}{(\sqrt{-\Xi}\tan(\frac{1}{2}\Omega\sqrt{-\Xi})+\beta)\sqrt{2w\epsilon(\Xi)}}\right)-\frac{c_1}{m}, \quad (50)$$

(38)

$$\mathbb{K}_{2,2}(x,t)=\pm\left(\frac{\sqrt{((n+(k-1)w)(1-k)}(\beta(\sqrt{-\Xi}\cot(\frac{1}{2}\Omega\sqrt{-\Xi})+\beta)-4\alpha\gamma)}{(\sqrt{-\Xi}\cot(\frac{1}{2}\Omega\sqrt{-\Xi})+\beta)\sqrt{2w\epsilon(\Xi)}}\right)e^{\iota(kx+et+\eta)}, \quad (51)$$

$$\mathbb{V}_{2,2}(x,t)=\frac{2cv}{m}\left(\frac{\sqrt{((n+(k-1)w)(1-k)}(\beta(\sqrt{-\Xi}\cot(\frac{1}{2}\Omega\sqrt{-\Xi})+\beta)-4\alpha\gamma)}{(\sqrt{-\Xi}\cot(\frac{1}{2}\Omega\sqrt{-\Xi})+\beta)\sqrt{2w\epsilon(\Xi)}}\right)-\frac{c_1}{m}, \quad (52)$$

$$\mathbb{K}_{2,3}(x,t)=\pm\left(\frac{\sqrt{((n+(k-1)w)(1-k)}(\beta(\sqrt{\Xi}\tanh(\frac{1}{2}\Omega\sqrt{\Xi})+\beta)-4\alpha\gamma)}{(\sqrt{-\Xi}\tanh(\frac{1}{2}\Omega\sqrt{\Xi})+\beta)\sqrt{2w\epsilon(\Xi)}}\right)e^{\iota(kx+et+\eta)}, \quad (53)$$

$$\mathbb{V}_{2,3}(x,t)=\frac{2cv}{m}\left(\frac{\sqrt{((n+(k-1)w)(1-k)}(\beta(\sqrt{\Xi}\tanh(\frac{1}{2}\Omega\sqrt{\Xi})+\beta)-4\alpha\gamma)}{(\sqrt{\Xi}\tanh(\frac{1}{2}\Omega\sqrt{\Xi})+\beta)\sqrt{2w\epsilon(\Xi)}}\right)-\frac{c_1}{m}, \quad (54)$$

$$\mathbb{K}_{2,4}(x,t)=\pm\left(\frac{\sqrt{((n+(k-1)w)(1-k)}(\beta(\sqrt{\Xi}\coth(\frac{1}{2}\Omega\sqrt{\Xi})+\beta)-4\alpha\gamma)}{(\sqrt{-\Xi}\coth(\frac{1}{2}\Omega\sqrt{\Xi})+\beta)\sqrt{2w\epsilon(\Xi)}}\right)e^{\iota(kx+et+\eta)}, \quad (55)$$

or

$$\mathbb{V}_{2,4}(x,t)=\frac{2cv}{m}\left(\frac{\sqrt{((n+(k-1)w)(1-k)}\left(\beta\left(\sqrt{\Xi}\coth\left(\frac{1}{2}\Omega\sqrt{\Xi}\right)+\beta\right)-4\alpha\gamma\right)}{\left(\sqrt{\Xi}\coth\left(\frac{1}{2}\Omega\sqrt{\Xi}\right)+\beta\right)\sqrt{2w\epsilon(\Xi)}}\right)^2e^{\iota(kx+wt+\eta)}-\frac{c_1}{m}. \quad (56)$$

DOI 10.2478/ama-2024-0064

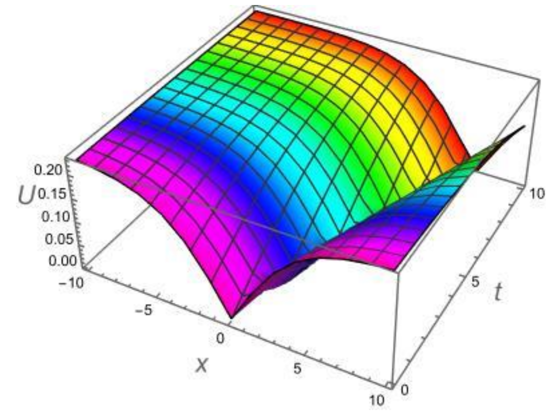

(a)

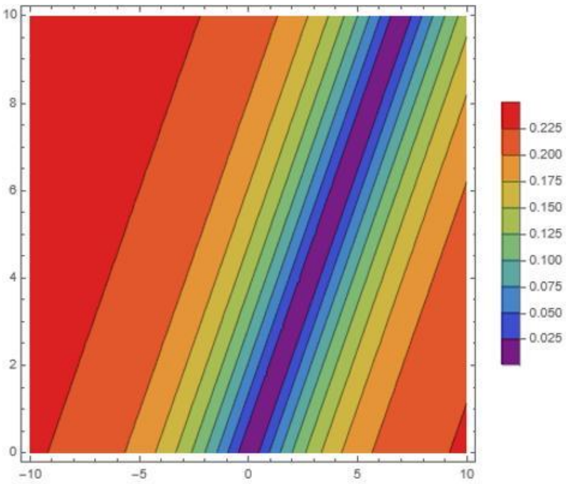

(b)

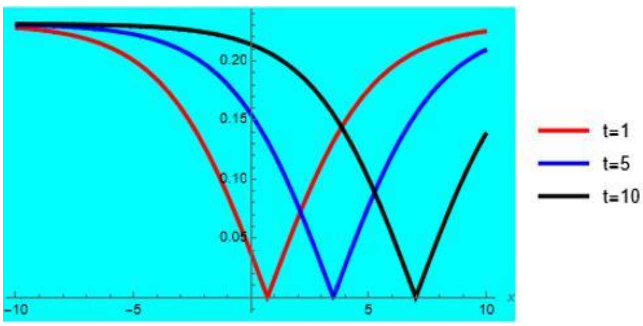

(c)

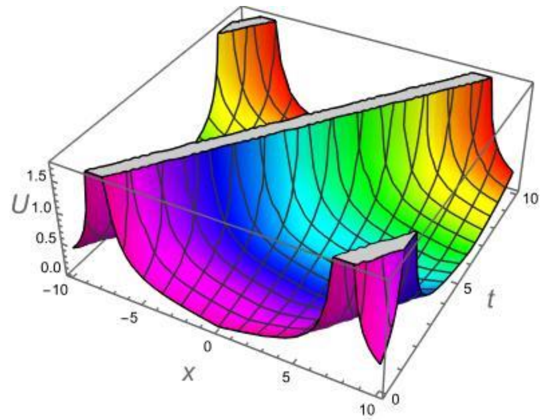

(d)

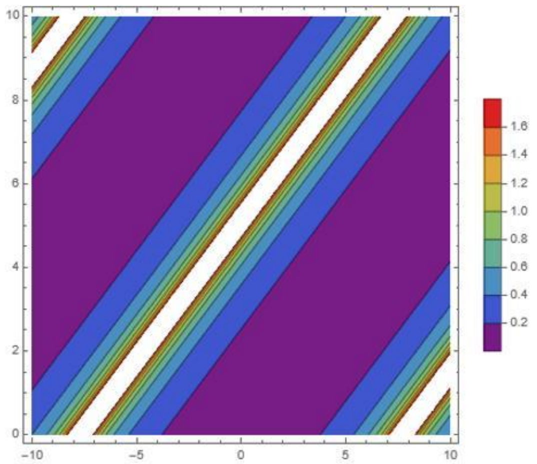

(e)

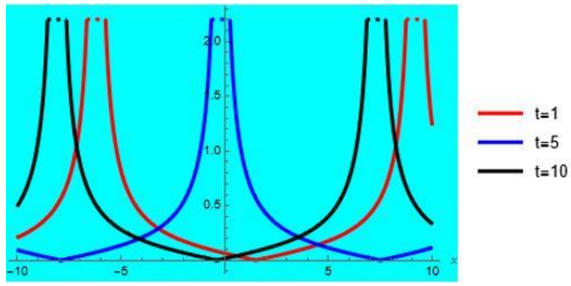

(f)

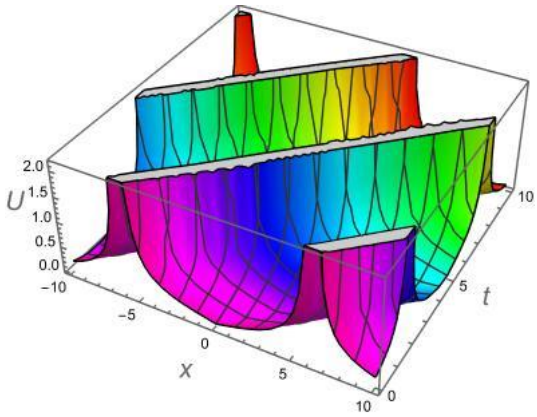

(g)

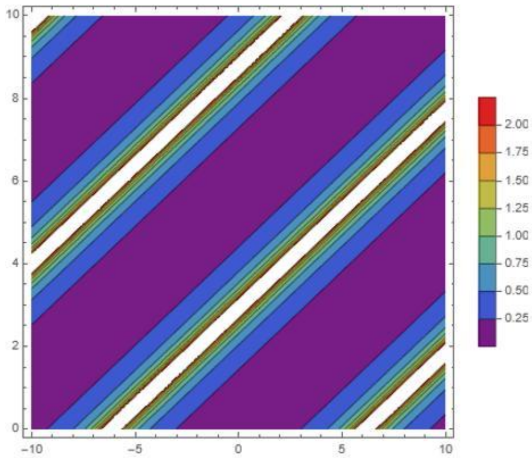

(h)

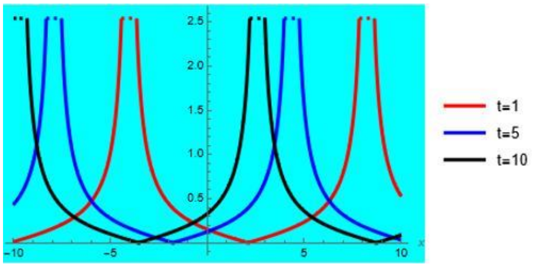

(i)

Fig. 1. Three-dimensional, contour and two-dimensional representations of the solution K1,1 across different parameter values of w. (a) 3-D visualisation at w = 0.35. (b) Contour visualisation at w = 0.35. (c) 2-D visualisation at w = 0.35. (d) 3-D visualisation at w = 0.75. (e) Contour visualisation at w = 0.75. (f) 2-D visualisation at w = 0.75. (g) 3-D visualisation at w = 1.05. (h) Contour visualisation at w = 1.05. (i) 2-D visualisation at w = 1.05

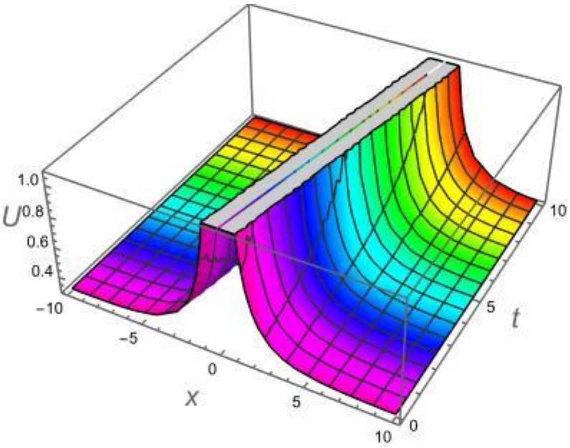

(a)

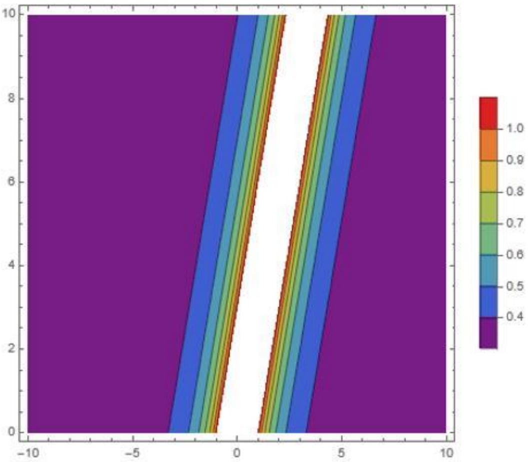

(b)

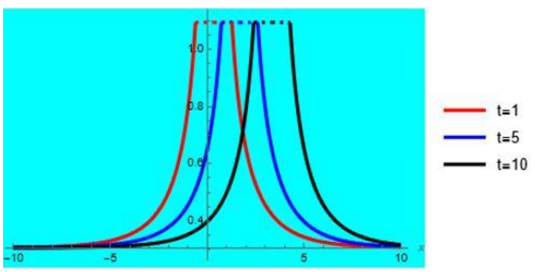

(c)

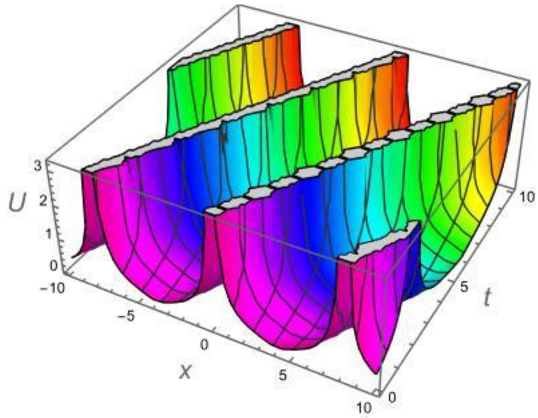

(d)

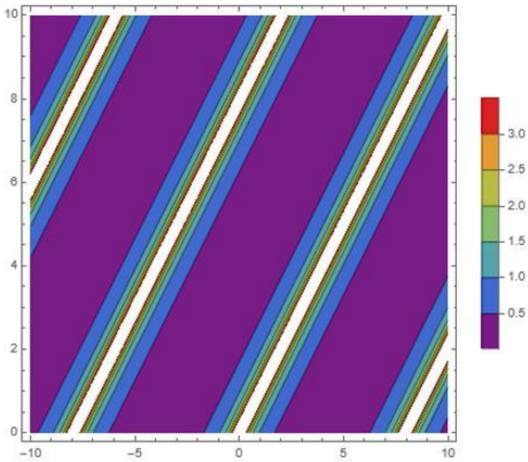

(e)

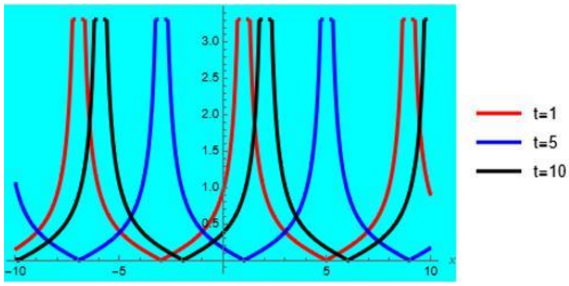

(f)

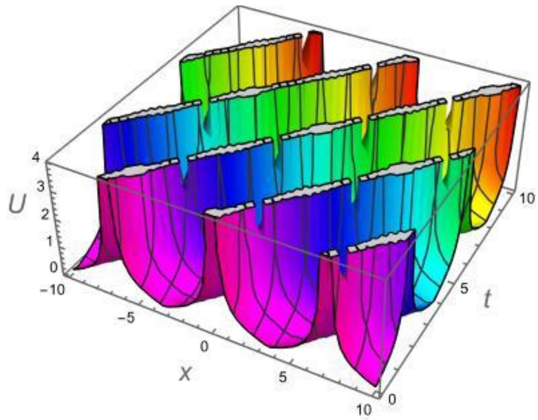

(g)

sciendo
DOI 10.2478/ama-2024-0064 acta mechanica et automatica, vol.18 no.4 (2024)

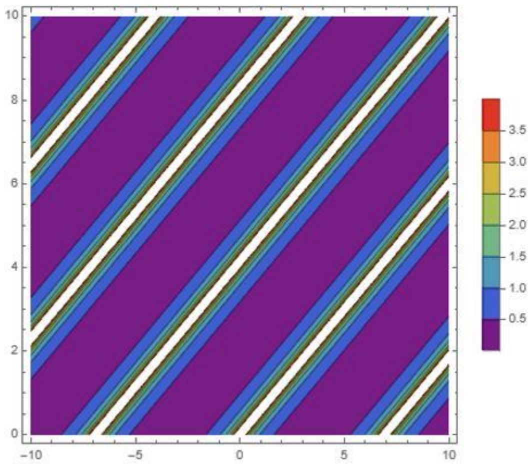

(h)

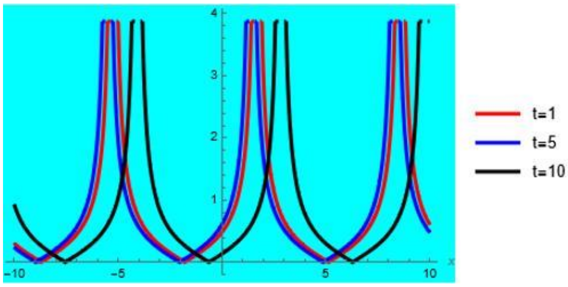

(i)

Fig. 2. Three-dimensional, contour and two-dimensional representations of the solution K1,4 across different values of w. (a) 3-D visualisation at w = 0.25. (b) Contour visualisation at w = 0.25. (c) 2-D visualisation at w = 0.25. (d) 3-D visualisation at w = 0.75 (e) Contour visualisation at w = 0.75 (f) 2-D visualisation at w = 0.75. (g) 3-D visualisation at w = 1.25. (h) Contour visualisation at w = 1.25. (i) 2-D visualisation at w = 1.25

3.2. Solution by applying Sardar sub-equation method

The solution using the Sardar sub-equation method for Eq. (35) can be expressed as follows, after determining the homogeneous balancing constant N = 1:

$$U(\Omega) = a_0 + a_1 M(\Omega) \quad (57)$$

To obtain the system of equations, the solution from Eq. (57) was substituted into Eq. (35), and the varying power coefficients of M(Ω) were calculated. The algebraic equation system that was obtained was then solved using the Mathematica software, which resulted in a family of values for a0, a1 and c. By Using this family, we got solutions as follows:

3.2.1. Family

$$a_0 = 0,\ a_1 = \pm\frac{\sqrt{(k-1)w+n}}{\sqrt{\upsilon w\epsilon}},\ c = \pm\frac{\sqrt{w(-(k-1)w-n)}}{\sqrt{\upsilon-k\upsilon}}. \quad (58)$$

General solution for family,

$$U(\Omega) = \frac{\sqrt{((n+(k-1)w)(1-k)}}{\sqrt{\upsilon w\epsilon}}M(\phi), \quad (59)$$

After using the general solution of Eq. (59) in Eqs (27) and (30), we get the following solutions: Case 1: if $\upsilon > 0$ and $\zeta = 0$;

$$\mathbb{K}_1(x,t) = \pm\sqrt{\frac{((n+(k-1)w)(1-k)pq}{w\epsilon}}(\mathrm{sech}_{pq}(\sqrt{\upsilon}\Omega))e^{\iota(kx+et+\eta)} \quad (60)$$

$$\mathbb{V}_1(x,t) = \frac{2\upsilon c}{m}(\sqrt{\frac{((n+(k-1)w)(1-k)pq}{w\epsilon}}(sech_{pq}(\sqrt{\upsilon}\Omega)))^2 e^{\iota(kx+wt+,eta)} - \frac{c_1}{m}, \quad (61)$$

$$\mathbb{K}_2(x,t) = \pm(\sqrt{\frac{((n+(k-1)w)(1-k)pq}{w\epsilon}}(\mathrm{csch}_{pq}(\sqrt{\upsilon}\Omega)))e^{\iota(kx+et+\eta)}, \quad (62)$$

$$\mathbb{V}_2(x,t) = \frac{2\upsilon c}{m}(\sqrt{\frac{((n+(k-1)w)(1-k)pq}{w\epsilon}}(\mathrm{csch}_{pq}(\sqrt{\upsilon}\Omega)))^2 e^{\iota(kx+wt+\eta)} - \frac{c_1}{m}. \quad (63)$$

Case 2: if $\upsilon < 0$ and $\zeta = 0$;

$$\mathbb{K}_3(x,t) = \pm(\sqrt{\frac{((n+(k-1)w)(1-k)pq}{w\epsilon}}(\mathrm{sec}_{pq}(\sqrt{-\upsilon}\Omega)))e^{\iota(kx+et+\eta)}, \quad (64)$$

$$\mathbb{V}_3(x,t) = \frac{2\upsilon c}{m}(\sqrt{\frac{((n+(k-1)w)(1-k)pq}{w\epsilon}}(\mathrm{sec}_{pq}(\sqrt{-\upsilon}\Omega)))^2 e^{\iota(kx+wt+\eta)} - \frac{c_1}{m}, \quad (65)$$

$$\mathbb{K}_4(x,t) = \pm(\sqrt{\frac{((n+(k-1)w)(1-k)pq}{w\epsilon}}(\mathrm{csc}_{pq}(\sqrt{-\upsilon}\Omega)))e^{\iota(kx+et+\eta)}, \quad (66)$$

$$\mathbb{V}_4(x,t) = \frac{2\upsilon c}{m}(\sqrt{\frac{((n+(k-1)w)(1-k)pq}{w\epsilon}}(\mathrm{csc}_{pq}(\sqrt{-\upsilon}\Omega)))^2 e^{\iota(kx+wt+\eta)} - \frac{c_1}{m}. \quad (67)$$

Case 3: if $\upsilon < 0$ and $\zeta = \frac{\upsilon^2}{4}$;

$$\mathbb{K}_5(x,t) = \pm(\sqrt{\frac{((n+(k-1)w)(k-1)}{2w\epsilon}}(\tan_{pq}(\sqrt{-\frac{\upsilon}{2}}\Omega)))e^{\iota(kx+et+\eta)}, \quad (68)$$

$$\mathbb{V}_5(x,t) = \frac{2c\upsilon}{m}\left(\sqrt{\frac{((n+(k-1)w)(k-1)}{2w\epsilon}}(\tan_{pq}(\sqrt{-\frac{\upsilon}{2}}\Omega))\right)^2 e^{\iota(kx+et+\eta)} - \frac{c_1}{m}, \quad (69)$$

$$\mathbb{K}_6(x,t) = \pm(\sqrt{\frac{((n+(k-1)w)(k-1)}{2w\epsilon}}(\coth_{pq}(\sqrt{-\frac{\upsilon}{2}}\Omega)))e^{\iota(kx+et+\eta)}, \quad (70)$$

$$\mathbb{V}_6(x,t) = \frac{2\upsilon c}{m}(\sqrt{\frac{(k-1)((k-1)w+n)}{2w\epsilon}}(\coth_{pq}(\sqrt{\frac{-\upsilon}{2}}\Omega)))^2 e^{\iota(kx+wt+\eta)} - \frac{c_1}{m}, \quad (71)$$

(59)

DOI 10.2478/ama-2024-0064

$$\mathbb{K}_7(x,t) = \pm(\sqrt{\frac{((n+(k-1)w)(k-1)}{2w\epsilon}}(\tanh_{pq}(\sqrt{-2\upsilon}\Omega)) \pm i\sqrt{-pq}\operatorname{sech}_{pq}(\sqrt{-2\upsilon}\Omega)))e^{\iota(kx+et+\eta)}, \tag{72}$$

$$\mathbb{V}_7(x,t) = \frac{2\upsilon c}{m}\left(\sqrt{\frac{(k-1)((k-1)w+n)}{2w\epsilon}}\left(\tanh_{pq}(\sqrt{-2\upsilon}\Omega) \pm \iota\sqrt{pq}\operatorname{sech}_{pq}(\sqrt{-2\upsilon}\Omega)\right)\right)^2 e^{\iota(kx+wt+\eta)} - \frac{c_1}{m}, \tag{73}$$

$$\mathbb{K}_8(x,t) = \pm(\sqrt{\frac{((n+(k-1)w)(k-1)}{2w\epsilon}}(\coth_{pq}(\sqrt{-2\upsilon}\Omega)) \pm i\sqrt{-pq}\operatorname{csch}_{pq}(\sqrt{-2\upsilon}\Omega)))e^{\iota(kx+et+\eta)}, \tag{74}$$

$$\mathbb{V}_8(x,t) = \frac{2\upsilon c}{m}\left(\sqrt{\frac{(k-1)((k-1)w+n)}{2w\epsilon}}\left(\coth_{pq}(\sqrt{-2\upsilon}\Omega) \pm \sqrt{pq}\operatorname{csch}_{pq}(\sqrt{-2\upsilon}\Omega)\right)\right)^2 e^{\iota(kx+wt+\eta)} - \frac{c_1}{m}, \tag{75}$$

$$\mathbb{K}_9(x,t) = \pm(\frac{1}{2}\sqrt{\frac{((n+(k-1)w)(k-1)}{2w\epsilon}}(\tanh_{pq}(\frac{1}{2}\sqrt{-\frac{\upsilon}{2}}\Omega)) \pm coth(\frac{1}{2}\sqrt{-\frac{\upsilon}{2}}\Omega)))e^{\iota(kx+et+\eta)}, \tag{76}$$

$$\mathbb{V}_9(x,t) = \frac{2\upsilon c}{m}(\frac{1}{2}\sqrt{\frac{(k-1)((k-1)w+n)}{2w\epsilon}}(\tanh_{pq}(\frac{1}{2}\sqrt{\frac{-\upsilon}{2}}\Omega) \pm \coth_{pq}(\frac{1}{2}\sqrt{\frac{-\upsilon}{2}}\Omega)))^2 e^{\iota(kx+wt+\eta)} - \frac{c_1}{m}. \tag{77}$$

Case 4: if υ > 0 and $\zeta = \frac{\upsilon^2}{4}$;

$$\mathbb{K}_{10}(x,t) = \pm(\sqrt{\frac{((n+(k-1)w)(1-k)}{2w\epsilon}}(\tanh_{pq}(\sqrt{\frac{\upsilon}{2}}\Omega)))e^{\iota(kx+et+\eta)}, \tag{78}$$

$$\mathbb{V}_{10}(x,t) = \frac{2c\upsilon}{m}\left(\sqrt{\frac{((n+(k-1)w)(1-k)}{2w\epsilon}}(\tanh_{pq}(\sqrt{\frac{\upsilon}{2}}\Omega))\right)^2 e^{\iota(kx+et+\eta)} - \frac{c_1}{m}, \tag{79}$$

$$\mathbb{K}_{11}(x,t) = \pm(\sqrt{\frac{((n+(k-1)w)(1-k)}{2w\epsilon}}(\cot_{pq}(\sqrt{\frac{\upsilon}{2}}\Omega)))e^{\iota(kx+et+\eta)}, \tag{80}$$

$$\mathbb{V}_{11}(x,t) = \frac{2\upsilon c}{m}(\sqrt{\frac{(n+w(k-1))(1-k)}{2w\epsilon}}(\cot_{pq}(\sqrt{\frac{\upsilon}{2}}\Omega)))^2 e^{\iota(kx+wt+\eta)} - \frac{c_1}{m}, \tag{81}$$

$$\mathbb{K}_{12}(x,t) = \pm(\sqrt{\frac{((n+(k-1)w)(1-k)}{2w\epsilon}}(\tan_{pq}(\sqrt{2\upsilon}\Omega)) \pm \sqrt{pq}\sec_{pq}(\sqrt{2\upsilon}\Omega)))e^{\iota(kx+et+\eta)}, \tag{82}$$

$$\mathbb{V}_{12}(x,t) = \frac{2\upsilon c}{m}\left(\sqrt{\frac{(n+w(k-1))(1-k)}{2w\epsilon}}\left(\tan_{pq}(\sqrt{2\upsilon}\Omega) \pm \sqrt{pq}\sec_{pq}(\sqrt{2\upsilon}\Omega)\right)\right)^2 e^{\iota(kx+wt+\eta)} - \frac{c_1}{m}, \tag{83}$$

$$\mathbb{K}_{13}(x,t) = \pm(\sqrt{\frac{((n+(k-1)w)(1-k)}{2w\epsilon}}(\cot_{pq}(\sqrt{2\upsilon}\Omega)) \pm \sqrt{pq}\csc_{pq}(\sqrt{2\upsilon}\Omega)))e^{\iota(kx+et+\eta)}, \tag{84}$$

$$\mathbb{V}_{13}(x,t) = \frac{2\upsilon c}{m}\left(\sqrt{\frac{(n+w(k-1))(1-k)}{2w\epsilon}}\left(\cot_{pq}(\sqrt{2\upsilon}\Omega) \pm \sqrt{pq}\csc_{pq}(\sqrt{2\upsilon}\Omega)\right)\right)^2 e^{\iota(kx+wt+\eta)} - \frac{c_1}{m}, \tag{85}$$

$$\mathbb{K}_{14}(x,t) = \pm(\frac{1}{2}\sqrt{\frac{((n+(k-1)w)(1-k)}{2w\epsilon}}(\tan_{pq}(\sqrt{\frac{\upsilon}{8}}\Omega)) \pm cot(\sqrt{\frac{\upsilon}{8}}\Omega)))e^{\iota(kx+et+\eta)}, \tag{86}$$

$$\mathbb{V}_{14}(x,t) = \frac{2\upsilon c}{m}\left(\frac{1}{2}\sqrt{\frac{(n+w(k-1))(1-k)}{w\epsilon}}\left(\tan_{pq}\left(\sqrt{\frac{\upsilon}{8}}\Omega\right) + \cot_{pq}\left(\sqrt{\frac{\upsilon}{8}}\Omega\right)\right)\right)^2 e^{\iota(kx+wt+\eta)} - \frac{c_1}{m}. \tag{87}$$

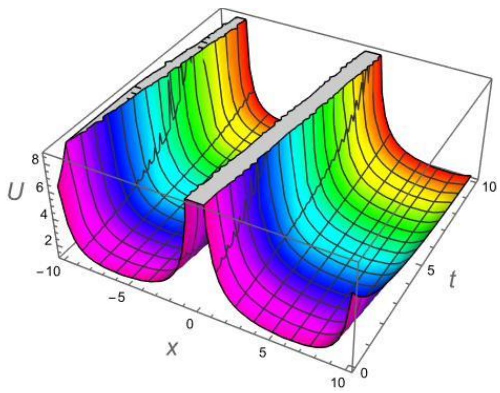

(a)

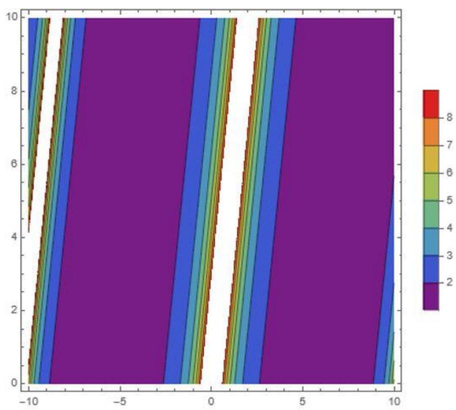

(b)

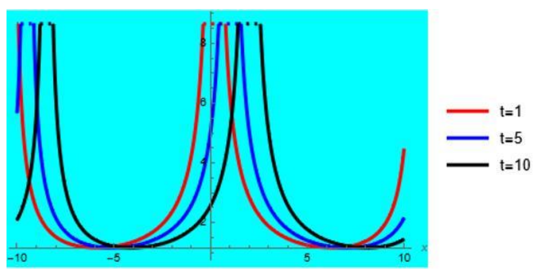

DOI 10.2478/ama-2024-0064

(c)

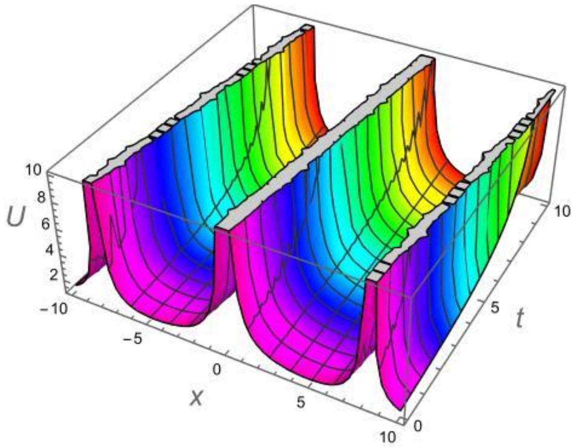

(d)

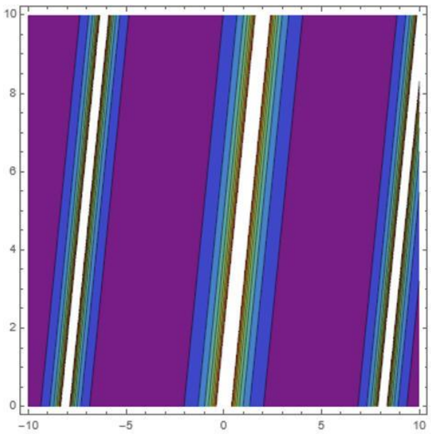

(e)

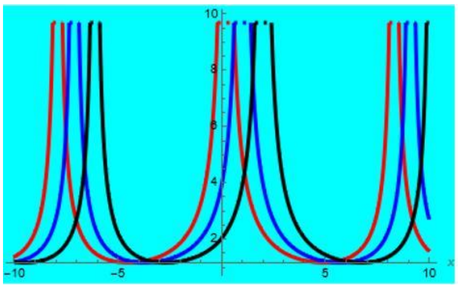

(f)

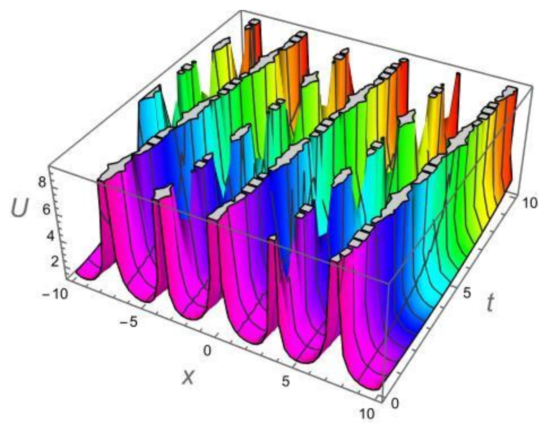

(g)

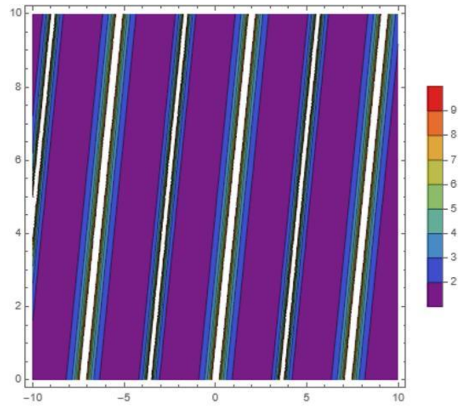

(h)

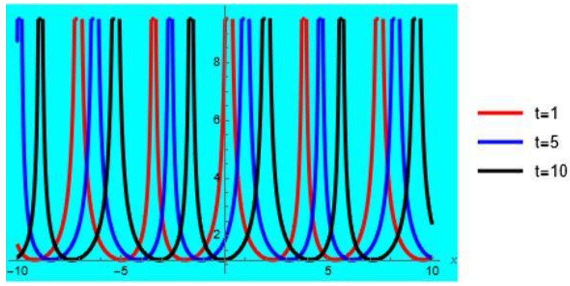

(i)

Fig. 3. Three-dimensional, contour and two-dimensional representations of the solution K8 across different parameter values of υ. (a) 3-D visualisation at υ = −1.25. (b) Contour visualisation at υ = −1.25. (c) 2-D visualisation at υ = −1.25. (d) 3-D visualisation at υ = −0.75. (e) Contour visualisation υ = −0.75. (f) 2-D visualisation υ = −0.75. (g) 3-D visualisation υ = −0.15. (h) Contour visualisation υ = −0.15. (i) 2-D visualisation υ = −0.15

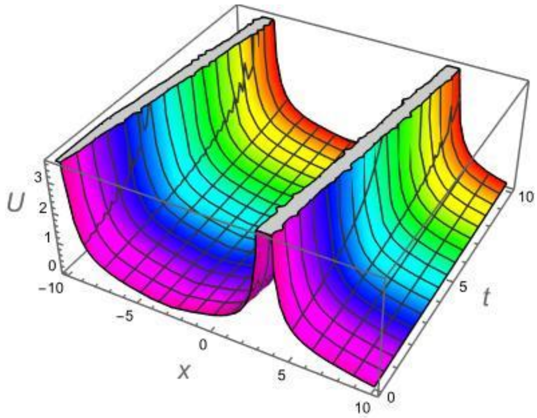

(a)

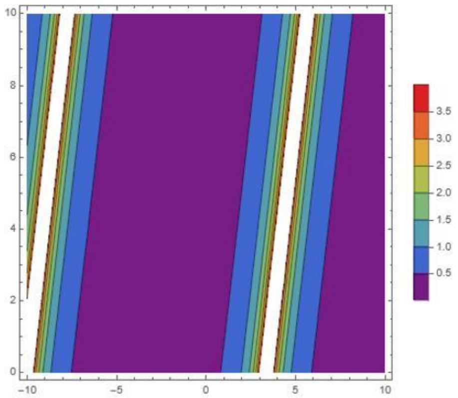

 DOI 10.2478/ama-2024-0064

(b)

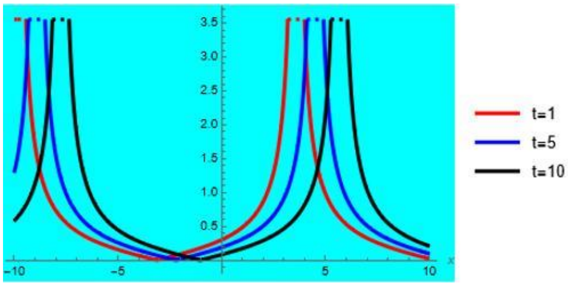

(c)

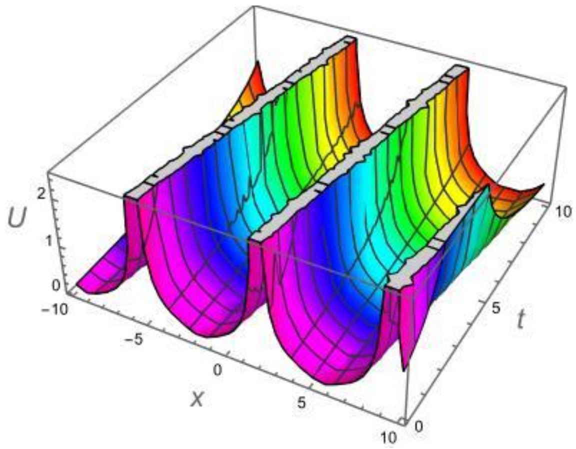

(d)

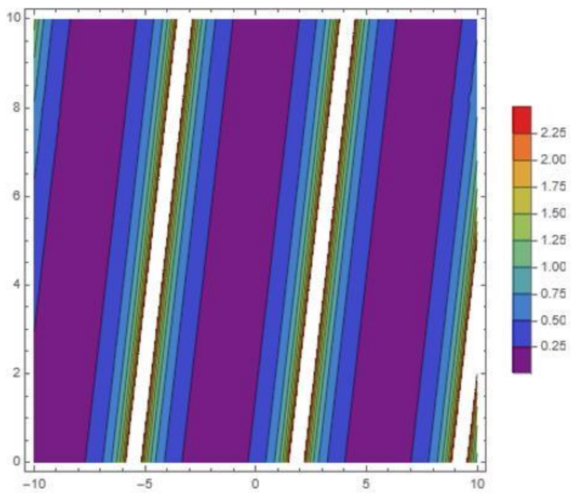

(e)

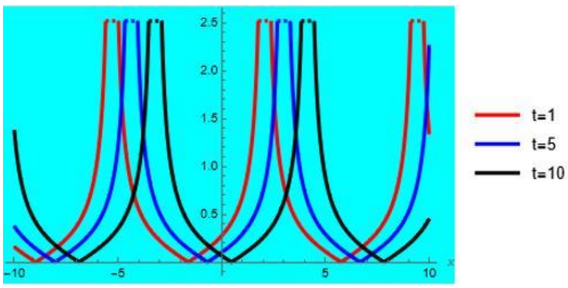

(f)

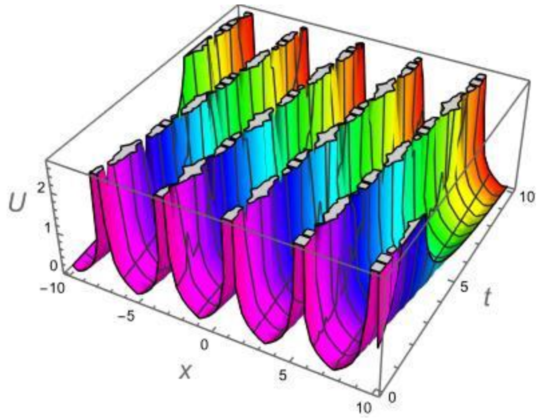

(g)

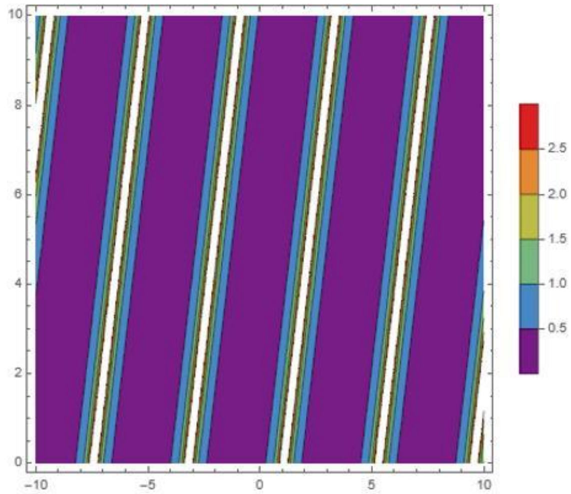

(h)

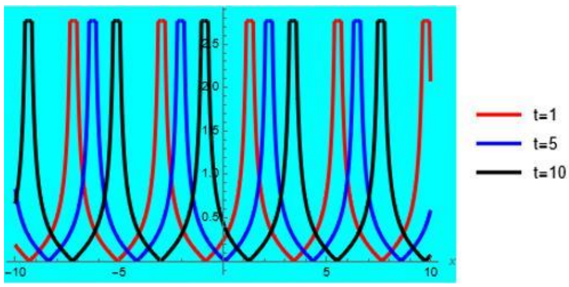

(i)

Fig. 4. Three-dimensional, contour and two-dimensional representations of the solution K12 across different parameter values of υ. (a) 3-D visualisation at υ = 0.5. (b) Contour visualisation at υ = 0.5. (c) 2-D visualisation at υ = 0.5. (d) 3-D visualisation at υ = 0.15, (e) Contour visualisation at υ = 0.15. (f) 2-D visualisation at υ = 0.15. (g) 3-D visualisation at υ = 0.05. (h) Contour visualisation at υ = 0.05. (i) 2-D visualisation at υ = 0.05

4. GRAPHICAL DISCUSSION

The purpose of this section is to provide a visual examination of the obtained results and their relevance in terms of physical implications.

Fig. 1 illustrates the transmission behaviour of the solution K1,1 at designated parameter values, α = 0.25, γ = 0.5, k = 0.5, β = 0.1 and n = 0.25. This solution anticipates an anti-kink periodic pattern exhibited by a travelling soliton, where the frequency rises as the parameter w increases. Fig. 2 illustrates the transmission behaviour of the solution K1,4 at designated parameter values, α = 0.25, γ = 0.5, k = 0.5, β = 0.1 and n = 0.25. This solution anticipates an anti-kink periodic pattern exhibited by a travelling soliton, where the frequency rises as the parameter w increases.

Fig. 3 shows the propagating behaviour of the solution K8 at designated parameter values, w = 15, k = 0.5, n = 0.25, p = 0.26 and q = 0.25. The proposed solution can forecast the behaviour of a travelling soliton that displays periodic patterns characterised by anti-peaked crests and anti-troughs. Furthermore, the frequency of this pattern is observed to increase as the value of the parameter υ increases.

Fig. 4 shows the propagating behaviour of the solution K12 at designated parameter values, w = 0.15, k = 0.35, n = 0.15, p = 0.52 and q = 0.5. The proposed solution can forecast the behaviour of a travelling soliton that displays periodic patterns characterised by anti-peaked crests and anti-troughs. Furthermore, the frequency of this pattern is observed to increase as the value of the parameter υ increases.

5. CONCLUSION

In this study, numerous novel solitons to the Kuralay equation are constructed through use of the modified auxiliary equation approach and the Sardar sub-equation method. Thus, numerous types of solitons such as a plane solution, periodic-stumpons, compacton, smooth soliton, multi-smooth kink, mixed-hyperbolic, periodic and mixed-periodic, compacton with singular peaks, mixed-trigonometric, trigonometric solution, peakon soliton, anti-peaked with decay, mixed-shock singular, mixed-singular, and singular and shock wave solutions are developed which are more generalised than the existing results. The propagation of solitons is graphically displayed in 3-D, contour and 2-D visualisation. The observed wave propagation displayed diverse behaviours, encompassing periodic patterns featuring elevated crests and troughs, as well as anti-peaked crests and troughs, periodic kinks, anti-kinks and compactons in both bright and dark forms. It is observed that the wave number is responsible to control the propagation of a solitary wave. Some appropriate values are selected for the involved free parameters in order to enlighten the graphical behaviour of the optical pulses using the developed analytical solutions. In interpreting the physical perspective of the nonlinear model, the proposed solutions may be considered to be authoritative. The modified auxiliary equation approach and the Sardar sub-equation method is a reliable and effective mathematical technique that can be applied to propose the analytical solutions to a number of other difficult physical phenomena. Additionally, there is potential to broaden the scope of this study to encompass lump interactions, multiple solitons and rogue wave breathers, thus expanding its practical utility.

REFERENCES

1. Iqbal MA, Wang Y, Miah MM, Osman MS. Study on date–Jimbo–Kashiwara–Miwa equation with conformable derivative dependent on time parameter to find the exact dynamic wave solutions. Fractal and Fractional. 2021;6(1):4.
2. Eidinejad Z, Saadati R, Li C, Inc M, Vahidi J. The multiple exp-function method to obtain soliton solutions of the conformable Date–Jimbo–Kashiwara–Miwa equations. International Journal of Modern Physics B. 2023;2450043.
3. Singh S, Ray SS. Integrability and new periodic, kink-antikink and complex optical soliton solutions of (3+ 1)-dimensional variable coefficient DJKM equation for the propagation of nonlinear dispersive waves in inhomogeneous media. Chaos, Solitons & Fractals. 2023;168:113184.
4. Majid SZ, Faridi WA, Asjad MI, Abd El-Rahman M, Eldin SM. Explicit soliton structure formation for the Riemann wave equation and a sensitive demonstration. Fractal and Fractional. 2023;7(2):102.
5. Muhamad KA, Tanriverdi T, Mahmud AA, Baskonus HM. Interaction characteristics of the Riemann wave propagation in the (2+ 1)-dimensional generalized breaking soliton system. International Journal of Computer Mathematics. 2023;100(6):1340-55.
6. Skipp J, Laurie J, Nazarenko S. Hamiltonian derivation of the point vortex model from the two-dimensional nonlinear Schrödinger equation. Physical Review E. 2023;107(2):025107.
7. Wang KJ, Liu JH. Diverse optical solitons to the nonlinear Schrödinger equation via two novel techniques. The European Physical Journal Plus. 2023 Jan;138(1):1-9.
8. Rizvi ST, Seadawy AR, Ahmed S, Bashir A. Optical soliton solutions and various breathers lump interaction solutions with periodic wave for nonlinear Schrödinger equation with quadratic nonlinear susceptibility. Optical and Quantum Electronics. 2023;55(3):286.
9. Asjad MI, Inc M, Faridi WA, Bakar MA, Muhammad T, Rezazadeh H. Optical solitonic structures with singular and non-singular kernel for nonlinear fractional model in quantum mechanics. Optical and Quantum Electronics. 2023;55(3):219.
10. Abu Bakar M, Owyed S, Faridi WA, Abd El-Rahman M, Sallah M. The First Integral of the Dissipative Nonlinear Schrödinger Equation with Nucci's Direct Method and Explicit Wave Profile Formation. Fractal and Fractional. 2022;7(1):38.
11. Akinyemi L, Şenol M, Osman MS. Analytical and approximate solutions of nonlinear Schrödinger equation with higher dimension in the anomalous dispersion regime. Journal of Ocean Engineering and Science. 2022;7(2):143-54.
12. Bruè E, De Lellis C. Anomalous dissipation for the forced 3D Navier–Stokes equations. Communications in Mathematical Physics. 2023;400(3):1507-33.
13. Hess MW, Quaini A, Rozza G. A data-driven surrogate modeling approach for time-dependent incompressible Navier-Stokes equations with dynamic mode decomposition and manifold interpolation. Advances in Computational Mathematics. 2023;49(2):22.
14. Lange T. Regularization by noise of an averaged version of the Navier–Stokes equations. Journal of Dynamics and Differential Equations. 2023;1-26.
15. Bruè E, De Lellis C. Anomalous dissipation for the forced 3D Navier–Stokes equations. Communications in Mathematical Physics. 2023;400(3):1507-33.
16. Wu XH, Gao YT, Yu X, Ding CC, Li LQ. Modified generalized Darboux transformation and solitons for a Lakshmanan-Porsezian-Daniel equation. Chaos, Solitons & Fractals. 2022;162:112399.
17. AA AQ, AM B, ASHF M, AA A, HO B. Dark and singular cubic–quartic optical solitons with Lakshmanan–Porsezian–Daniel equation by the improved Adomian decomposition scheme. Ukrainian Journal of Physical Optics. 2023;24(1).
18. Faridi WA, Asjad MI, Jarad F. Non-linear soliton solutions of perturbed Chen-Lee-Liu model by Φ 6-model expansion approach. Optical and Quantum Electronics. 2022;54(10):664.
19. Khater MM, Zhang X, Attia RA. Accurate computational simulations of perturbed Chen–Lee–Liu equation. Results in Physics. 2023;45:106227.
20. Khatun MM, Akbar MA. New optical soliton solutions to the space-time fractional perturbed Chen-Lee-Liu equation. Results in Physics. 2023;46:106306.
21. Kumar S, Niwas M. New optical soliton solutions and a variety of dynamical wave profiles to the perturbed Chen–Lee–Liu equation in optical fibers. Optical and Quantum Electronics. 2023;55(5):418.

22. Qureshi ZA, Bilal S, Khan U, Akgül A, Sultana M, Botmart T, Zahran HY, Yahia IS. Mathematical analysis about influence of Lorentz force and interfacial nano layers on nanofluids flow through orthogonal porous surfaces with injection of SWCNTs. Alexandria Engineering Journal. 2022;61(12):12925-41.
23. Shah IA, Bilal S, Akgül A, Tekin MT, Botmart T, Zahran HY, Yahia IS. On analysis of magnetized viscous fluid flow in permeable channel with single wall carbon nano tubes dispersion by executing nano-layer approach. Alexandria Engineering Journal. 2022;61(12): 11737-51.
24. Faridi WA, Asjad MI, Jarad F. The fractional wave propagation, dynamical investigation, and sensitive visualization of the continuum isotropic bi-quadratic Heisenberg spin chain process. Results in Physics. 2022;43:106039.
25. Asjad MI, Faridi WA, Jhangeer A, Ahmad H, Abdel-Khalek S, Alshehri N. Propagation of some new traveling wave patterns of the double dispersive equation. Open Physics. 2022;20(1):130-41.
26. Almusawa H, Jhangeer A. A study of the soliton solutions with an intrinsic fractional discrete nonlinear electrical transmission line. Fractal and Fractional. 2022;6(6):334.
27. Asjad MI, Faridi WA, Jhangeer A, Aleem M, Yusuf A, Alshomrani AS, Baleanu D. Nonlinear wave train in an inhomogeneous medium with the fractional theory in a plane self-focusing.
28. Fahim MR, Kundu PR, Islam ME, Akbar MA, Osman MS. Wave profile analysis of a couple of (3+ 1)-dimensional nonlinear evolution equations by sine-Gordon expansion approach. Journal of Ocean Engineering and Science. 2022;7(3):272-9.
29. Liu JG, Osman MS. Nonlinear dynamics for different nonautonomous wave structures solutions of a 3D variable-coefficient generalized shallow water wave equation. Chinese Journal of Physics. 2022;77:1618-24.
30. Baber MZ, Seadway AR, Iqbal MS, Ahmed N, Yasin MW, Ahmed MO. Comparative analysis of numerical and newly constructed soliton solutions of stochastic Fisher-type equations in a sufficiently long habitat. International Journal of Modern Physics B. 2023; 37(16): 2350155.
31. Kumar S, Niwas M. Optical soliton solutions and dynamical behaviours of Kudryashov's equation employing efficient integrating approach. Pramana. 2023;97(3):98.
32. Kumar S, Niwas M. Abundant soliton solutions and different dynamical behaviors of various waveforms to a new (3+ 1)-dimensional Schrödinger equation in optical fibers. Optical and Quantum Electronics. 2023;55(6):531.
33. Niwas M, Kumar S. New plenteous soliton solutions and other form solutions for a generalized dispersive long-wave system employing two methodological approaches. Optical and Quantum Electronics. 2023;55(7):630.
34. El-Ganaini S, Kumar S, Niwas M. Construction of multiple new analytical soliton solutions and various dynamical behaviors to the nonlinear convection-diffusion-reaction equation with power-law nonlinearity and density-dependent diffusion via Lie symmetry approach together with a couple of integration approaches. Journal of Ocean Engineering and Science. 2023;8(3):226-37.
35. Kumar S, Niwas M, Dhiman SK. Abundant analytical soliton solutions and different wave profiles to the Kudryashov-Sinelshchikov equation in mathematical physics. Journal of Ocean Engineering and Science. 2022;7(6):565-77.
36. Abdou MA, Ouahid L, Kumar S. Plenteous specific analytical solutions for new extended deoxyribonucleic acid (DNA) model arising in mathematical biology. Modern Physics Letters B. 2023;37(34): 2350173.
37. Kumar S, Kumar A. A study of nonlinear extended Zakharov–Kuznetsov dynamical equation in (3+ 1)-dimensions: Abundant closed-form solutions and various dynamical shapes of solitons. Modern Physics Letters B. 2022;36(25):2250140.
38. Mathanaranjan T. New Jacobi elliptic solutions and other solutions in optical metamaterials having higher-order dispersion and its stability analysis. International Journal of Applied and Computational Mathematics. 2023;9(5):66.
39. Mathanaranjan T. Optical solitons and stability analysis for the new (3+ 1)-dimensional nonlinear Schrödinger equation. Journal of Nonlinear Optical Physics & Materials. 2023;32(02):2350016.
40. Zhao YH, Mathanaranjan T, Rezazadeh H, Akinyemi L, Inc M. New solitary wave solutions and stability analysis for the generalized (3+ 1)-dimensional nonlinear wave equation in liquid with gas bubbles. Results in Physics. 2022;43:106083.
41. Mathanaranjan T, Kumar D, Rezazadeh H, Akinyemi L. Optical solitons in metamaterials with third and fourth order dispersions. Optical and Quantum Electronics. 2022;54(5):271.
42. Mathanaranjan T, Vijayakumar D. New soliton solutions in nanofibers with space-time fractional derivatives. Fractals. 2022;30(07): 2250141.
43. Mathanaranjan T, Hashemi MS, Rezazadeh H, Akinyemi L, Bekir A. Chirped optical solitons and stability analysis of the nonlinear Schrödinger equation with nonlinear chromatic dispersion. Communications in Theoretical Physics. 2023;75(8):085005.
44. Hosseini K, Hincal E, Salahshour S, Mirzazadeh M, Dehingia K, Nath BJ. On the dynamics of soliton waves in a generalized nonlinear Schrödinger equation. Optik. 2023;272:170215.
45. Aksoy A, Yenikaya S. Soliton wave parameter estimation with the help of artificial neural network by using the experimental data carried out on the nonlinear transmission line. Chaos, Solitons & Fractals. 2023;169:113226.
46. Khater MM. Computational and numerical wave solutions of the Caudrey–Dodd–Gibbon equation. Heliyon. 2023;9(2).
47. Al Alwan B, Abu Bakar M, Faridi WA, Turcu AC, Akgül A, Sallah M. The Propagating Exact Solitary Waves Formation of Generalized Calogero–Bogoyavlenskii–Schiff Equation with Robust Computational Approaches. Fractal and Fractional. 2023;7(2):191.
48. Khater MM. A hybrid analytical and numerical analysis of ultra-short pulse phase shifts. Chaos, Solitons & Fractals. 2023;169:113232.
49. Ozdemir N, Secer A, Bayram M. Extraction of soliton waves from the longitudinal wave equation with local M-truncated derivatives. Optical and Quantum Electronics. 2023;55(4):313.
50. Zahran EH, Bekir A, Ibrahim RA, Sagidullayeva Z, Myrzakulov R. New diverse types of the soliton arising from the integrable Kuralay equations against its numerical solutions.
51. Zahran EH, Bekir A. Unexpected configurations for the optical solitons propagation in lossy fiber system with dispersion terms effect. Mathematical Methods in the Applied Sciences. 2023;46(4):4055-69.
52. Zahran EH, Bekir A. New unexpected behavior to the soliton arising from the geophysical Korteweg–de Vries equation. Modern Physics Letters B. 2022;36(08):2150623.
53. Raheel M, Zafar A, Ali MR, Myrzakulova Z, Bekir A, Myrzakulov R. New analytical wave solutions to the M-fractional Kuralay-II equations based on three distinct schemes.
54. Mathanaranjan T. Optical soliton, linear stability analysis and conservation laws via multipliers to the integrable Kuralay equation. Optik. 2023;290:171266.
55. Bettelheim E, Smith NR, Meerson B. Inverse scattering method solves the problem of full statistics of nonstationary heat transfer in the Kipnis-Marchioro-Presutti model. Physical Review Letters. 2022;128(13):130602.
56. Gonzalez-Gaxiola O, Biswas A, Ekici M, Khan S. Highly dispersive optical solitons with quadratic–cubic law of refractive index by the variational iteration method. Journal of Optics. 2022;1-8.
57. Al-Tai MH, Al-Fayadh A. Solving two dimensional coupled Burger's equations using transform variational iteration method. InAIP Conference Proceedings 2023; 2414(1):040030. AIP Publishing LLC.
58. Zhang Y, Dang S, Li W, Chai Y. Performance of the radial point interpolation method (RPIM) with implicit time integration scheme for transient wave propagation dynamics. Computers & Mathematics with Applications. 2022;114:95-111.
59. Zagorac JL, Sands I, Padmanabhan N, Easther R. Schrödinger-Poisson solitons: Perturbation theory. Physical Review D. 2022;105(10):103506.

60. He XJ, Lü X. M-lump solution, soliton solution and rational solution to a (3+ 1)-dimensional nonlinear model. Mathematics and Computers in Simulation. 2022;197:327-40.
61. Aniqa A, Ahmad J. Soliton solution of fractional Sharma-Tasso-Olever equation via an efficient (G'/G)-expansion method. Ain Shams Engineering Journal. 2022;13(1):101528.
62. Kumar S, Malik S, Rezazadeh H, Akinyemi L. The integrable Boussinesq equation and it's breather, lump and soliton solutions. Nonlinear Dynamics. 2022;1-4.
63. Akram G, Sadaf M, Zainab I. Bright, dark, periodic and kink solitary wave solutions of evolutionary Zoomeron equation. Authorea Preprints. 2022.
64. Asjad MI, Munawar N, Muhammad T, Hamoud AA, Emadifar H, Hamasalh FK, Azizi H, Khademi M. Traveling wave solutions to the Boussinesq equation via Sardar sub-equation technique. AIMS Mathematics. 2022;7(6):11134-49.

This work was supported by the Ministry of Science and Higher Education of the Republic of Kazakhstan, Grant AP14870191.

Waqas Ali Faridi: https://orcid.org/0000-0003-0713-5365

Muhammad Abu Bakar: https://orcid.org/0000-0003-3903-098X

Zhaidary Myrzakulova: https://orcid.org/0000-0002-4047-4484

Ratbay Myrzakulov: https://orcid.org/0000-0002-5274-0815

Mawahib Elamin: https://orcid.org/0000-0002-7907-4672

Lakhdar Ragoub: https://orcid.org/0000-0001-8747-1814

Lanre Akinyemi: https://orcid.org/0000-0002-5920-250X